ORIGINAL ARTICLE
DOI: 10.5433/1679-0375.2022v43n1p45

Max-Min fairness-based resource allocation in massive MIMO systems

Alocação de recursos baseada em imparcialidade Max-Min para sistemas MIMO massivos

Marcelo Henrique Jeronymo[1]; Taufik Abrão[2]

Abstract

This work deals with power and spectrum allocation approaches for massive MIMO (M-MIMO) systems. An analysis is made to verify the efficiency of the solutions provided by schemes used for the spectral and energy efficiency (SE-EE) trade-off problem in massive antenna-based wireless communication systems. We first introduce the *Geometry Based Stochastic Model* (GBSM) channel model (One-ring model), describing the behavior of a uniform linear array of antennas (ULA) arrangement, revealing how the channel parameters affect the channel capacity. We also show that under this model, the SE still increases without boundary when the massive number of base-station (BS) antennas M increases, provided that pilot contamination is substantially mitigated or eliminated but when the number of users equipment (UEs) K increases with a fixed number of antennas in the BS, there is a increasing limitation from the combiners in mitigating the inter-user interference, making decoding difficult. The downlink (DL) M-MIMO scenario is analyzed, by introducing the generalized power allocation problem and derived the max-min fairness scheme from it. We propose a procedure to solve the max-min problem and made conclusions about the algorithmic solution in terms of complexity and respective EE and SE performance.

Keywords: Massive MIMO; resource allocation; energy efficiency; spectral efficiency; Max-min fairness.

Resumo

Este trabalho trata de abordagens de alocação de potência e espectro para sistemas múltiplas entradas e múltiplas saídas massivo (M-MIMO). É feita uma análise para verificar a eficiência das soluções fornecidas pelos esquemas usados para o problema de trade-off espectral e de eficiência energética (SE-EE) em sistemas de comunicação sem fio baseados em antenas massivas. Primeiro apresentamos o modelo de canal estocástico baseado em geometria (GBSM), descrevendo o comportamento de um arranjo linear uniforme de antenas (ULA), e mostramos como os parâmetros do canal afetam a capacidade do canal. Também mostramos que, sob este modelo, o SE ainda aumenta sem limites quando o número M de antenas de estação base (BS) aumenta, desde que a contaminação do piloto seja substancialmente mitigada ou eliminada, mas quando o número K de usuários (UEs) aumenta com um número fixo de antenas na BS, há uma limitação crescente dos combinadores em mitigar a interferência inter-usuário, dificultando a decodificação. O cenário de downlink (DL) é analisado, introduzindo o problema generalizado de alocação de energia e derivando o esquema de max-min a partir dele. Propomos um procedimento para resolver o problema max-min e interpretamos a solução algorítmica em termos de complexidade e respectivo desempenho EE e SE.

Palavras-chave: Potência; espectro; MIMO massivo; alocação de potência; justiça Max-Min; modelo de canal estocástico geométrico.

[1] Undergraduated student, Electrical Engineering Department, UEL, Londrina, Paraná, Brazil; E-mail: marcelo.henrique@uel.br
[2] Prof. Dr., Electrical Engineering Department; UEL, Londrina, Paraná, Brazil; E-mail: taufik@uel.br

Introduction

With such a high growth rate of connected devices each year, fifth-generation (5G) wireless communication systems must provide coverage and capacity for all of these devices, while improving the user experience and traffic rates. For this reason, communication systems of multiple transmitting and receiving antennas (MIMO - *multiple input multiple output*) have become quite popular due to the many benefits they can achieve, including diversity of transmission and high data rates. To match these requirements resources such as spectrum and power need be allocated in a suitable and reliable way, since such resources are quite limited.

The concept of *extra large* MIMO (XL-MIMO) arises through the implementation of large physical *arrays*, that is, a system implemented through numerous antennas, where it can be applied in places of large infrastructures such as airports, stadiums, etc. This feature is similar that found in M-MIMO systems. However, there are some peculiar characteristics, which differ from M-MIMO systems, including the channel non-stationary in addition to the concept of *visibility region* (VR). Such characteristics become evident when analyzing how the transmission is carried out when there is an array of antennas not only with a larger number of antennas compared to M-MIMO but with an antenna spacing greater than usual. Studies show that assumptions as flat wave model used in M-MIMO are not feasible when there is a scattering in the physical size of the array, requiring the implementation of spherical wave models (BJORNSON *et al*., 2019; JENG-SHIANN; INGRAM, 2005; PAYAMI; TUFVESSON, 2012; ZHOU ZHOU; FANG; CHEN, 2015)

Elaborating further on the key feature associated to XL-MIMO, the *visibility region* (VR) is a physical region of the array in which most (or all) of the signal strength is concentrated; such separation of parts of the array occurs due to obstacles, trees, constructions, etc., hindering the signal propagation. Finally, spatial *non-stationary channel* in wireless systems is when the visibility of a UE is dynamic, which changes according to the intrinsic movement of users. Studies show how these phenomena impact on the signal processing tasks, such as the spherical wave modeling and the impact on linear receivers performance (ALI; CARVALHO; HEATH, 2019; CARVALHO *et al*., 2020). In general, M-MIMO system modeling assume spatial *stationary* for the most practical channel scenarios.

In the context of the wireless system, one fundamental design that should be considered is the effect of pilot contamination on the performance of M-MIMO and extra-large (XL) MIMO systems. In Sanguinetti, Bjornson and Hoydis (2020) the authors demonstrate that the appropriate exploration of the spatial correlation propagation and by using suitable signal processing schemes that eliminate interference one can eliminate the upper bounds on capacity, and consequently eliminate the upper bound on spectral efficiency (SE).

The resource allocation (RA) approach, including power allocation in downlink (DL) or uplink (UL) transmissions. Today there are many power allocation schemes available in the literature, such as *Max-min fairness*, *Max-sum SE* and *Max-product SINR*. The idea is to maximize a utility function subject to a constraint, which can be one of the three schemes mentioned above. Hence there are studies investigating how to improve the algorithm's performance used to solve such RA problems, since it is necessary to attain quickly convergence before UE's location changes. Notice that even a problem with posynomial complexity (which the usual approach schemes deployed currently) can take longer to solve in such small channel coherence interval.

A novel power allocation algorithm to maximize the spectral efficiency (SE) and energy efficiency (EE) of MIMO broadcast channels under individual quality of service (QoS) constraints is devised in Kwon *et al*. (2020). To address the impact of delay outage, effective capacity (EC), *i.e.*, the maximum constant arrival rate satisfying statistical delay-QoS constraint is considered. Using such a performance metric, effective-EE and EC are formulated as a bi-objective optimization power allocation problem with QoS constraints. Salh *et al*. (2019) considers a low-complexity energy efficiency scheme aiming to allocate transmit power in downlink (DL) direction based on Newton optimization method and Lagrange decomposition. This algorithm was used to provide the optimal EE for massive MIMO systems. Besides, in Li *et al*. (2019) the authors propose an iterative algorithm that solves the power allocation problem in conjunction with antenna selection. The algorithm is based in Lagrangian dual problem used in a single cell M-MIMO scenario. The proposed scheme outperforms existing schemes.

The contributions of the paper are threefold. First, we formulate and discuss suitable resource allocation problems for M-MIMO systems operating under linear combiners/precoding. Second, we propose an effective Max-min-based algorithm solution for power allocation problems

in M-MIMO systems. Third, the effectiveness of the algorithmic solution in terms of performance-complexity trade-off is extensively confirmed by numerical results.

The remainder of this paper is organized as follows. The second section describes the adopted M-MIMO system model. The third section discusses three power allocation schemes for M-MIMO systems considering DL transmissions. The fourth section presents a numerical results analysis demonstrating the efficiency and effectiveness of the proposed PA solutions. The last section concludes the paper.

M-MIMO system model

An M-MIMO communication system can be defined as a network of *base stations* (BS) and *users* or *user equipment* (*UE*) with a L amount of cells. Each BS is equipped with M antennas and is responsible for covering a cell with K UEs (BJORNSON; HOYDIS; SANGUINETTI, 2017). Some important features includes: a) Use of the *Space-Division Multiple Access* method (*SDMA*), allowing to manage several UEs in the same time-frequency resources; b) The BS contains more antennas than UEs in its respective cell, with a proportion of $M/K \geq 4$ for better performance when using SDMA, with $M \geq 64$, although some authors use the canonical way of defining a M-MIMO network with $M/K \geq 1$ (BJORNSON; HOYDIS; SANGUINETTI, 2017); c) Operates with TDD (*Time-Division Duplex*) protocol for data transmission and reception; d) Linear processing for data recovery with M-MMSE estimator/receiver.

The concept of Massive MIMO applies when the number of BS antennas grows beyond 64, separated by at least by the carrier wavelength $\lambda/2$. In such configuration, one can see two fundamental properties of *M-MIMO*, namely *channel hardening* and *favorable propagation*, respectively, defined as (BJORNSON; HOYDIS; SANGUINETTI, 2017);

$$\frac{||\mathbf{h}_{jk}^{j}||^2}{\mathbb{E}\{||\mathbf{h}_{jk}^{j}||^2\}} \to 1 \quad \text{(channel hardenning)}$$

$$\frac{(\mathbf{h}_{li}^{j})^H \mathbf{h}_{jk}^{j}}{\sqrt{\mathbb{E}\{||\mathbf{h}_{li}^{j}||^2\}\mathbb{E}\{||\mathbf{h}_{jk}^{j}||^2\}}} \to 0 \quad \text{(favorable propagation)}$$

almost surely as $M \to \infty$. In other words, channel hardening is a property that allows the channel to approach a deterministic channel, as can be proved that $\mathbb{V}\left\{\frac{||\mathbf{h}_{jk}^{j}||^2}{\mathbb{E}\{||\mathbf{h}_{jk}^{j}||^2\}}\right\}$ goes to 0, and favorable propagation means that two UEs with $\mathbf{h}_{li}^{j}$ and $\mathbf{h}_{jk}^{j}$ channels, will become orthogonal, as the numerator $(\mathbf{h}_{jk}^{j})^H \mathbf{h}_{jk}^{j}$ goes to 0 and $(\cdot)^H$ is the conjugate transpose operation.

UL and DL communication

There are two types of transmission, *Uplink* (UL) and *Downlink* (DL), the first refers to the transmission of data from the UEs to the BS, the second refers to the transmission from the BS to the UEs of the cell. Let's consider a single-cell system; in the UL transmission, the BS antennas captures the received signal represented by a vector, given in equation (1):

$$\mathbf{y} = \sum_{k=1}^{K} \mathbf{h}_k s_k + \mathbf{n}, \tag{1}$$

where $\mathbf{y} \in \mathbb{C}^M$, the $s_k \sim \mathscr{CN}(0, p_k)$ is the signal sent by the kth UE with p_k being the power transmitted, and $\mathbf{h}_k$ representing the channel response which models the path between the kth UE and the BS in the cell. The channel response is modeled according to the type of propagation and the existence of line-of-sight (LoS) or not (NLoS). Herein we assume the following NLoS model, equation (2):

$$\mathbf{h}_{lk}^{j} \sim \mathscr{CN}(\mathbf{0}_M, \mathbf{R}_{lk}^{j}). \tag{2}$$

For the DL communication direction, in j-th cell the BS first applies a precoding vector $\mathbf{w}_i$, to the signal, and transmits the signal over M antennas as in beams, represented by equation (3):

$$\mathbf{x} = \sum_{i=1}^{K} \mathbf{w}_i \varsigma_i, \tag{3}$$

where $\mathbf{w}_{jk} \in \mathbb{C}^M$ is the precoding vector, determining the spatial direction of transmission. This vector provides the spacial user separability, satisfying the normalization $\mathbb{E}\{\|\mathbf{w}_{jk}\|^2\} = 1$. Besides, $\varsigma_i \sim \mathscr{CN}(0, \rho_i)$ is the modulated signal that is transmitted by the BS for the ith UE with ρ_i being the average power transmitted by it, such that $\mathbb{E}\{\|\mathbf{w}_i \varsigma_i\|^2\} = \rho_i$ (BJORNSON; HOYDIS; SANGUINETTI, 2017).

The received signal at the k UE in cell j can be represented by three terms: desired signal, interference, and noise, as:

$$\begin{aligned} y_k &= \sum_{l=1}^{L} (\mathbf{h}_k)^H \mathbf{x} + n_k \\ &= \underbrace{(\mathbf{h}_k)^H \mathbf{w}_k \varsigma_k}_{\text{Desired signal}} + \underbrace{\sum_{\substack{i=1 \\ i \neq k}}^{K} (\mathbf{h}_k)^H \mathbf{w}_i \varsigma_i}_{\text{Interference from the cell}} + n_k \end{aligned}$$

where $n_k \sim \mathscr{CN}(0, \sigma_{\text{DL}}^2)$ is the downlink independent noise with variance σ_{DL}^2.

TDD protocol

In this protocol, UL and DL transmissions are contained in blocks in the Time × Frequency plane, a coherence block. Where T is the period of time where the channel response can be considered constant over time and B is the bandwidth which the channel can be considered constant over frequency.

The product bandwidth-symbol period $\tau_c = B \cdot T$ is described by the quantity of the number of data symbols possible to be transmitted inside a coherence block.

Channel model for M-MIMO systems

To make an analysis of M-MIMO systems, it is important to represent how the medium between the UEs and the BS of a cell behaves. First, we introduce the *GBSM model, Geometry Based Stochastic Model*. The complexity of the model is higher than CBSM models, *Correlation Based Stochastic Model*, but can describe much better the behavior of the system (OLIVERAS MARTINEZ; EGGERS; CARVALHO, 2016; ZHENG; OU; YIN, 2014). In this work, we use a 2D-GBSM model, namely One-ring to describe the behavior of a uniform linear array of antennas (ULA). The channel response is expressed by eqaution (4)

$$\mathbf{h}_k \to \mathscr{N}_{\mathbb{C}}(\mathbf{0}_M, \mathbf{R}_k), \quad N_{path} \to \infty \tag{4}$$

where N_{path} denotes the multiple components of k UE in cell l to BS j and the channel correlation matrix is defined as:

$$[\mathbf{R}_k]_{m,n} = \beta \int e^{2\pi d_H (m-n) sin(\bar{\varphi})} f(\bar{\varphi}) d\bar{\varphi}, \quad \bar{\varphi} = \varphi + \Delta, \tag{5}$$

Δ is the angle of spread given in radians, f($\bar{\varphi}$) is the PDF (*probability density function*) of $\bar{\varphi}$, β is the large-scale pathloss coefficient, being modeled as:

$$\beta_k = \Upsilon_{ref} - 10\alpha \log_{10}\left(\frac{d_k}{1\,km}\right) \quad \text{[dB]}$$

$$\Upsilon_{ref} = -148 \quad \text{[dB]}$$

For the *One-Ring* channel model we consider the spread angle Δ to be a uniform distribution expressed by equation (6)

$$\Delta \sim \mathscr{U}(-\delta, \delta), \qquad \text{with} \quad f(\Delta) = \frac{1}{2\delta}, \tag{6}$$

where $f(\Delta)$ denotes the PDF of Δ. The parameter δ is related to the standard deviation of the spread angle, *i.e.*, $\sigma_\Delta = 0.577 \cdot \delta$. Using equation (5) with (6) we have

$$[\mathbf{R}]_{m,n} = \frac{\beta}{2\Delta} \int_{-\Delta}^{\Delta} e^{2\pi d_H (m-n) sin(\varphi+\delta)} d\delta. \tag{7}$$

Using equation (7), one can generate a channel response vector by evaluating equation (8)

$$\mathbf{h}_k = \mathbf{R}_k^{\frac{1}{2}} \mathbf{e}, \tag{8}$$

where vector $\mathbf{e} \sim \mathscr{N}_{\mathbb{C}}(\mathbf{0}_M, I_M)$. This expression is known by Karhunen-Loeve expansion (BJORNSON; HOYDIS; SANGUINETTI, 2017).

Combiners

To extract data from a UE, the BS needs to efficiently estimate the channel response ($\mathbf{h}_k$), this can be done by using the *minimum mean-squared error* (MMSE) channel estimator from which an estimated channel response $\hat{\mathbf{h}}_k$ is generated. In this paper we assume perfect channel estimation, or simply put: $\hat{\mathbf{h}}_k = \mathbf{h}_k$, and aiming to make each equation more compact, we use $\mathbf{V} = [\mathbf{v}_1\ \mathbf{v}_2\ \cdots\ \mathbf{v}_K]$ where each column represents the combiner from cell to kth UE.

1) Maximum-ratio combiner (MRC): The combiner MR aims to maximize the received SNR by multiplying the received signal by the channel matrix defined as in equation (9)

$$\mathbf{V}^{\text{MR}} = \hat{\mathbf{H}}^H \tag{9}$$

2) Zero forcing (ZF) combiner: The goal of ZF combining scheme is to eliminate the interference caused by other UEs in the same cell. The expression to compute the ZF detector is given by equation (10)

$$\mathbf{V}^{\text{ZF}} = \hat{\mathbf{H}}((\hat{\mathbf{H}})^H \hat{\mathbf{H}})^{-1}, \tag{10}$$

3) M-MMSE combiner: The M-MMSE combination scheme is more efficient than the previous one, due to the fact that it takes into account the interference not only between UEs of the same cell, but also outside it, however, such efficiency requires greater computational complexity. The expression to compute the M-MMSE detector is given by equation (11)

$$\mathbf{V}^{\text{M-MMSE}} = \left(\hat{\mathbf{H}}\mathbf{P}(\hat{\mathbf{H}})^H + \sum_{i=1}^{K} p_i C_i + \sigma_{\text{UL}}^2 I_M\right)^{-1}, \tag{11}$$

where $\mathbf{P}$ = diag(p_1, p_2, $\cdots$, p_K) is the power diagonal matrix where each element (in the main diagonal) is the power transmitted from each UE.

Spectral Efficiency

The spectral efficiency (*SE*) is a measure of the average number of bits of information per complex-valued sample that it can be reliably transmit over the channel (BJORNSON; HOYDIS; SANGUINETTI, 2017).

An ergodic lower bound for the system SE can be evaluated as in equation (12)

$$\underline{\mathrm{SE}}_k^{\mathrm{UL,DL}} = \frac{\tau_{u,d}}{\tau_c}\log_2\left(1+\underline{\mathrm{SINR}}_k^{\mathrm{UL,DL}}\right), \qquad (12)$$

where $\tau_{u,d}$ is the samples used in UL or DL transmission. Considering the UL transmission, the effective $\underline{\mathrm{SINR}}$ can be expressed as equation (13)

$$\underline{\mathrm{SINR}}_k^{\mathrm{UL}} = \frac{p_k a_k}{\sum_{i=1}^{K} p_i b_{ki} - p_k a_k + \sigma_{\mathrm{UL}}^2 \mathbb{E}\{||\mathbf{v}_k||^2\}}, \qquad (13)$$

where $a_k = |\mathbb{E}\{\mathbf{v}_k^H \mathbf{h}_k\}|^2$ and $b_{ki} = \mathbb{E}\{|\mathbf{v}_k^H \mathbf{h}_i|^2\}$.

Now considering the DL transmission, an ergodic lower bound for the $\mathrm{SE}_{jk}^{\mathrm{DL}}$ can be evaluated by deploying the following effective $\underline{\mathrm{SINR}}$, equation (14)

$$\underline{\mathrm{SINR}}_k^{\mathrm{DL}} = \frac{\rho_k a_k}{\sum_{i=1}^{K} \rho_i b_{ki} - \rho_k a_k + \sigma_{\mathrm{DL}}^2}, \qquad (14)$$

where $a_k = |\mathbb{E}\{\mathbf{w}_k^H \mathbf{h}_k\}|^2$ and $b_{ik} = \mathbb{E}\{|\mathbf{w}_i^H \mathbf{h}_k|^2\}$, and then evaluating, equation (12), with $\tau_{u,d} = \tau_d$. The same applies for UL.

The $\underline{\mathrm{SINR}}_{jk}^{\mathrm{UL}}$ in equation (13) defines the lower bound for the capacity of kth UE in the jth cell. As expected, it depends on $\mathbf{h}_{jk}$, which is a random variable. We apply the expectation as indicated in equation (13) across different coherence blocks. Indeed, one can evaluate the SE by taking the mean value of $\log_2\left(1+\mathrm{SINR}_{jk}^{\mathrm{UL}}\right)$ using numerical Monte Carlo simulation (MCS) method, where the $\mathrm{SINR}_{jk}^{\mathrm{UL}}$ is evaluated at each channel realization in each coherence block.

Energy Efficiency

Energy Efficiency (EE) is a metric of efficiency in wireless and greed wireless communications that computes the number of bits that a system can reliably transmit per unit of energy (BJORNSON; HOYDIS; SANGUINETTI, 2017), and defined by equation (15)

$$\eta_{\mathrm{EE}} = \frac{\eta_{\mathrm{SE}}}{\mathrm{P_{RF}} + \mathrm{P_{CIRC}}}, \qquad (15)$$

where

$$\eta_{\mathrm{SE}} = B\sum_{k=1}^{K} \underline{\mathrm{SE}}_k^{\mathrm{UL}} + \underline{\mathrm{SE}}_k^{\mathrm{DL}}, \qquad (16)$$

$$\mathrm{P_{RF}} = \frac{(\tau_p+\tau_u)}{\tau_c}\sum_{k=1}^{K}\frac{1}{\mu_{\mathrm{UE},k}}p_k + \frac{\tau_d}{\tau_c}\frac{1}{\mu_{\mathrm{BS}}}\sum_{k=1}^{K}\rho_k, \qquad (17)$$

$$\mathrm{P_{CIRC}} = P_{\mathrm{FIX}} + M\cdot P_{\mathrm{BS}}. \qquad (18)$$

The η_{SE} parameter in equation (15) is associated to the system throughput; the $\mathrm{P_{RF}}$ is the effective transmitted RF power by the base-station, with each $\mu_{\mathrm{UE,K}}$ and μ_{BS} being the efficiency of the *power amplifier* (PA), taking values in between $\mu \in [0;1]$. Finally, the P_{CIRC} is the *circuit power* consumption of the system, splitted in a fixed parcel and another associated per BS antenna consumption (P_{BS}).

Power allocation strategies

In this section we discuss the three most used schemes for power allocation to the UEs in DL transmissions. As stated before, our objective is to maximize a certain utility function defined as in equation (19)

$$\mathrm{U}(\mathrm{SE}_{11}^{\mathrm{DL}},...,\mathrm{SE}_{LK_L}^{\mathrm{DL}}) = \begin{cases} a)\ \sum_{j=1}^{L}\sum_{k=1}^{K_j}\mathrm{SE}_{jk} & \text{or} \\ b)\ \min_{j,k}\mathrm{SE}_{jk} & \text{or} \\ c)\ \prod_{j=1}^{L}\prod_{k=1}^{K_j}\mathrm{SINR}_{jk} \end{cases} \qquad (19)$$

Such utility functions in equation (19) can be identified as: *a) Max-sum SE*; *b) Max-min fairness*; *c) Max-prod SINR*.

The goal is optimize a specific utility function U subject to the power budget and formulated as in equation (20)

$$\underset{\rho_{11}\geq 0,...,\rho_{LK_L}\geq 0}{\text{maximize}}\ \mathrm{U}(\mathrm{SE}_{11}^{\mathrm{DL}},...,\mathrm{SE}_{LK_L}^{\mathrm{DL}}); \qquad (20)$$
$$\text{subject to}\ \sum_{k=1}^{K_j}\rho_{jk} \leq P_{\mathrm{MAX}}^{\mathrm{DL}},\ \ j=1,...,L,$$

where $P_{\mathrm{MAX}}^{\mathrm{DL}}$ is the available power available at the BS. Hence, the constraint in equation (20) represents the total power transmitted by BS j serving K_j UEs.

Each utility function gives a different result in between the maximum SE and fairness performance.The *Max-min SE* scheme tries to establish all UEs to almost equal SE, making the most fairness scheme, but lacks throughput in the network since UEs with better channel conditions to improve SE will be neglected to make the UEs with poor channel conditions get a higher SE. On the other hand, the *Max-sum SE* power allocation scheme searches for the maximum throughput with a cost in fairness; in this scheme, some UEs may have close to zero SE, consequently impacting UEs with poor channel conditions. Finally, the *Max-prod SINR* scheme is somewhat a balance in between these previous schemes, seeking to find a good system throughput and good fairness simultaneously, since under such PA scheme the SINR of all users is multiplied together. Besides, under this PA scheme, one cannot afford to hold UEs with low SINR, otherwise it will affect negatively the attempt to maximize the utility function. Also, since the Max-prod scheme is derived from Max-sum SE, by neglecting the 1 inside the log function and

using log proprieties, this manipulation leads to a higher SE for the weakest UEs (BJORNSON *et al.*, 2019). Many optimization methods can be used to effectively solve the optimization problem. A detailed analysis on the generalized convex optimization problems is given in Boyd and Vandenberghe (2004).

Solving the Max-min fairness PA problem in M-MIMO

To solve the *Max-min fairness* power allocation problem in M-MIMO systems, we need to change the optimization statement to one we can work with. By reformulating the original *Max-min fairness* subproblem b) in equation (19), results:

$$\begin{aligned} \gamma^{\star} \;=\; & \underset{\rho_1\geq 0,\ldots,\rho_K\geq 0,\gamma\geq 0}{\text{maximize}}\ \gamma \\ \text{s.t. } & \sum_{k=1}^{K}\rho_k \leq P^{\text{DL}}, \\ & \text{SINR}_k \geq\ \gamma,\ k=1,...,K \end{aligned} \tag{21}$$

where $\gamma^{\star}$ is the optimal SINR found as the result of maximizing the minimum SINR, γ. To solve equation (21), one can split the optimization problem in two subproblems, the first one consists in optimizing γ. We approach this using a *bisection* method by halving the search space each iteration and making γ a fixed parameter while solving the second sub-problem, that consists in finding a feasible power vector ρ that satisfies the power budget constraint in equation (21). Besides, each power-candidate vector results in a set of SINR that must satisfies the second constraint in equation (21). The Algorithm 1 describes how to approach the problem computationally.

Algorithm 1 Bisection algorithm

1: **procedure** MAXMINFAIRNESS($a_i, b_{ik}, P^{DL}_{\max}, \varepsilon, \sigma^2_{DL}$)
2: $\quad\gamma_{lower} \leftarrow 0$
3: $\quad\gamma_{upper} \leftarrow \min\left(\frac{P^{DL}_{\max} a_i}{\sigma^2_{DL}}\right), \forall i \in 1,\ldots,K$
4: $\quad\rho^{\star} \leftarrow \mathbf{0}$
5: $\quad$**while** $\gamma_{upper} - \gamma_{lower} > \varepsilon$ **do**
6: $\quad\quad\gamma_{cand.} \leftarrow (\gamma_{lower} + \gamma_{upper})/2$
7: $\quad\quad\triangleright$ Search for a solution using (21) restrictions
8: $\quad\quad$**if** Feasible **then**
9: $\quad\quad\quad\gamma_{lower} \leftarrow \gamma_{cand.}$
10: $\quad\quad\quad\rho^{\star} \leftarrow \rho_{sol.}$
11: $\quad\quad$**else**
12: $\quad\quad\quad\gamma_{upper} \leftarrow \gamma_{cand.}$
13: $\quad$**return** $\rho^{\star}$

First we begin by initializing γ_{lower} and γ_{upper}, where the $\min\left(\frac{P^{DL}_{\max} a_i}{\sigma^2_{DL}}\right), \forall i$ represents the minimum SINR among all users under maximum power allocated and no interference. These variables define the lower and upper bounds, respectively, in the search region that the algorithm will search a feasible solution; besides, the initial solution vector $\rho^{\star} = \mathbf{0}$ is defined. After that, the boundaries for difference of the upper and lower SINR is reduced in each new iteration; the iterations stop when these SINR difference becomes less than ε. Line 6 defines the middle point between the two extremes and try to establish the new minimum SINR solution to be used in problem (21), i.e., find new power vector solution ρ, line 7 of the Algorithm 1. The algorithm used for this is provided by CVX-OPT library (ANDERSEN; DAHL; VANDENBERGHE, 2021), assuming that for each bisection step the resulting sub-problem is convex. Since the nature of the problem is linear, we used a cone linear programming algorithm based on Nesterov-Todd scaling (ANDERSEN; DAHL; VANDENBERGHE, 2021). If a solution is found, and it is feasible, then the lower SINR boundary is updated as the middle point $\gamma_{cand.}$ previously computed; on the other hand, if the solution is not found or the problem is infeasible, we simply update the γ_{upper} bound with the middle point γ_{cand}. The iterations stops when the two values γ_{lower} and γ_{upper} are sufficiently close together; hence, under such condition, the current power vector solution is the output optimal power solution, $\rho^{\star}$. Notice that line 7 in the Algorithm 1 represents the sub-problem two where does not need an objective function, only a feasible solution (one that satisfies all the constraints given) and can be solved, for instance, by using interior-points methods.

Numerical results

In this section, numerical analyses on which parameter values influence the correlated M-MIMO channel capacity and energy efficiency are discussed. We evaluates the SE in the UL and DL correlated M-MIMO channels, as well as the EE-SE tradeoff in M-MIMO. Besides, it is demonstrated numerically that when the number of antennas at the BS increases, the spectral efficiency in the uplink increases without boundary if in massive MIMO the pilot contamination could be substantially mitigated or even eliminated by using the MMSE combiner.

Uplink SE in M-MIMO

In this simulation we show that when the antennas at the BS increases, given a fixed value for UEs, the SE

increases without bound when using M-MMSE combining scheme. We also show that with a fixed number of antennas in the BS, there is so much UEs that the BS can support without decreasing the SE due to too much interference, in that sense if we are able to conjecture a optimal number of UEs for each cell, we can allocate the users in a multicell scenario accordingly with the number of antennas that each cell has in its BS so we can maximize the sum SE of the overall system. For this subsection, the parameter values adopted in the simulations are depicted in Table 1. The sum-SE results with varying number of BS antennas M are depicted in Figure 1. While results for the sum-SE *vs* number of UEs (K) are represented in Figure 2.

Table 1 – Adopted Parameters for SE analyses

Parameter	Figure 1	Figure 2	Figure 3
Δ	$\mathscr{U}(-\delta^\circ, \delta^\circ)$	$\mathscr{U}(-\delta^\circ, \delta^\circ)$	$\mathscr{U}(-\delta^\circ, \delta^\circ)$
δ°	15	[15;30;45]	45
AoA	$\mathscr{U}(-\frac{\pi}{2}, \frac{\pi}{2})$	$\mathscr{U}(-\frac{\pi}{2}, \frac{\pi}{2})$	$\mathscr{U}(-\frac{\pi}{2}, \frac{\pi}{2})$
M	[10:10:100]	64	64
K	16	[10:10:60]	16
realizations	100	100	100
τ_c	200	200	200
τ_p	16	K	16
τ_u	92	100 - K/2	92
p_{jk} (W)	1	0.1	0.1
$P_{\max}^{\mathrm{DL}}$ (mW)	–	–	$100 \cdot K$
σ^2 (W)	1	1	1

Source: The authors.

The SE behavior of system equipped with M-MMSE, ZF and MR combiners in UL transmission when the number of BS antennas M increases is analyzed in Figure 1. The SE using M-MMSE and ZF combiners in this scenario grows without bounds. This is not the case when using MR combiner, which can be seen that the SE grows much slower and does not attain substantial gain benefit (array gain) when the number of BS antennas increases.

For the M-MMSE combiner in Figure 2 one can notice that increasing the number of UEs K, the sum-SE grows until near $K \approx 40$ users then it starts to decrease with a slow slope. However, for the ZF combiner, such sum-SE growth almost like the M-MMSE combining, as expected, but the maximum is attained for $K \approx 25$ users; after that, the M-MIMO system equiped with ZF combiner starts to decay fast, and at a point where $50 \leq K \leq 60$ (near to full system loading $\mathscr{L} = \frac{K}{M} \to 1$), the curve is below the sum-SE using the MR combiner.

Figure 1 – SE as a function of the number of BS antennas, M.

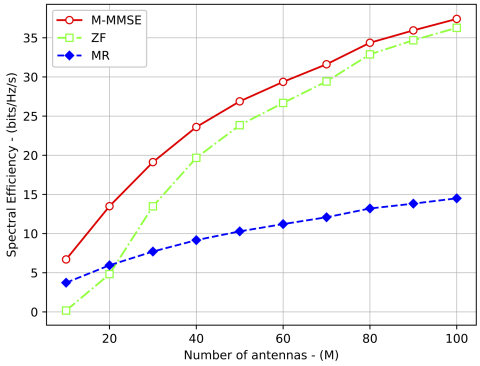

Source: The authors.

Finally, the MR combiner presents the worst sum-SE results, except when $K \geq 50$ users. This is because in ZF definition, the combiner aims to minimize noise and the interference of UEs, but when the interference becomes to much to be mitigated, *i.e.*, in case of full system loading or even when operating under over-crowed scenarios ($\mathscr{L} > 1$), the ZF combiner does not have the capacity to extract information from the signal since already it used its full capacity to mitigate interference.

Figure 2 – UL sum-SE as a function of the number of UEs, K and fixed number of BS antennas, $M = 64$.

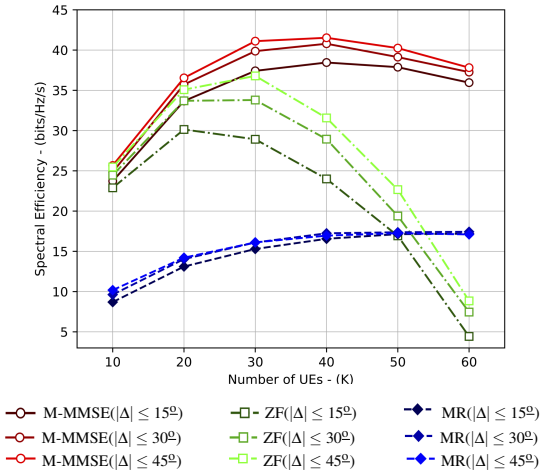

Source: The authors.

Downlink SE in M-MIMO

In this subsection the effects of using an optimization approach to provide power allocation of transmit signal at BS is analysed. By optimizing equation (21) for each precoder and ploting the DL sum-SE behavior allow us to get further insights. We do this using CVXOPT library for Python 3. Due the convexity of the problems, and using the formulation in equation (21), one can find a feasible solution given the power constraints with $P_{\max}^{\mathrm{DL}} = 100 \cdot K = 1600$ [mW].

Figure 3 confirms that using Max-min power allocation strategy reduces the sum-rate and overall SE compared to the equal power approach (EPA), as indicated in black lines. Indeed, when using max-min power allocation scheme, one can confirm the effectiveness in terms of increasing the minimum rate attained by any user in the system, being the CDF for the SE more abrupt in comparison with the equal power strategy (EPA). By plotting the CDF of multiples measurements of the SE in Figure 3, one can see that by using a power allocation scheme we can guarantee that all UEs will have at least a minimal amount of SE (improving the fairness) and using the same power as before, but at a cost of reducing the power being transmitted to UEs with good conditions. Hence decreasing the SE per user, and sum-rate, but increasing substantially the overall EE.

Figure 3 – Cumulative distribution function (CDF) for the DL per user SE: $Pr(\mathrm{SE}_k^{\mathrm{DL}} \leq \mathrm{SE}_0)$ under system loading $\mathscr{L} = 0.25$.

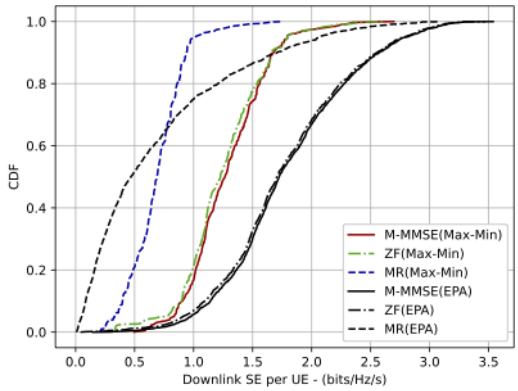

Source: The authors.

EE-SE tradeoff in M-MIMO

Let's consider the impact of power allocation scheme in the EE and SE improvement when using specifically the *Max-min fairness* procedure. By using both transmission directions (UL and DL), one can compute the system EE. Figure 4 depicts the system EE *vs* SE under different combiner/precoding influences. The parameter values adopted in these simulations are depicted in Table 2.

Each point in Figure 4 represents an increasing in the number of BS antennas, with step of 10 in the range: $M \in 10:10:100$ antennas at BS. One can see that either M-MMSE or ZF can perform well in terms of EE-SE when $M \approx 30$ to ≈ 40 antennas; once again, MR combiner/precoding does not have a sufficient benefit for using as much as available number of antennas to improve substantially either EE or SE, despite its advantage of reduced complexity among the techniques considered.

Table 2 – Adopted Parameters for EE-SE trade-off analysis

Parameter	Figure 4	Parameter	Figure 4
Δ	$\mathscr{U}(-\delta^\circ, \delta^\circ)$	p_{jk} (W)	1
δ°	$\frac{\pi}{4}$	$P_{\max}^{\mathrm{DL}}$ (W)	1.6
AoA	$\mathscr{U}(-\frac{\pi}{2}, \frac{\pi}{2})$	P_{FIX} (W)	1
M	[10:10:100]	P_{BS} (W)	0.5
K	16	B (MHz)	1
Realizations	100	$\mu_{\mathrm{UE},k}$	0.4
τ_c	200	μ_{BS}	0.6
τ_p	16	σ^2 (W)	1
τ_u	92	ε	0.005

Source: The authors.

Figure 4 – System EE *versus* SE, where each point represents a different number of antennas, M.

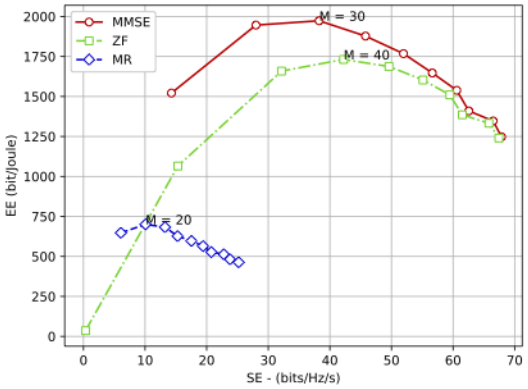

Source: The authors.

Complexity analysis

Let's consider the impact of using the proposed algorithm to solve optimization problem posed in equation (21). The parameter values deployed in this simulation setup are summarized in Table 3, while Figure 5 depicts the numerical results obtained by varying K users and M antennas, and measuring the execution time for each realization and taking the mean value from it.

Table 3 – Adopted parameters for complexity analysis. other parameter values are the same of Table 2

Parameter	Figure 5	Parameter	Figure 5
M	[10:10:70]	p_{jk} (W)	0.1
K	[10:10:60]	$P_{\max}^{\mathrm{DL}}$ (W)	$0.1 \cdot K$
τ_p	K	ε	0.01
τ_u	$100 - \frac{K}{2}$	σ^2 (W)	1

Source: The authors.

From Figure 5, one can infer that the time execution detection performance under MR and MMSE combiners are quite similar in terms of a linear growth in both dimensions K and M, including typical massive MIMO

scenarios for M and K, sharing approximately the same execution time. While using ZF combiner, the system attain the least amount of execution time to perform detection, ranging from 0 to 0.10 seconds (on average) but it does not growth linearly, since when $K = M$ one can observe the well-known singularity in the ZF detection behavior, attaining the lowest execution time, but it does not mean a valid solution; instead, for each iteration the cone programming algorithm return unfeasible solutions, and if most iterations are impractical, the algorithm converges faster but the solution found is not valid or as good as compared to MMSE combiner in the same full loading condition ($M = K$).

Figure 5 – Execution time for MIMO system under variable number of users and BS antennas, by using MR, ZF and MMSE combiners.

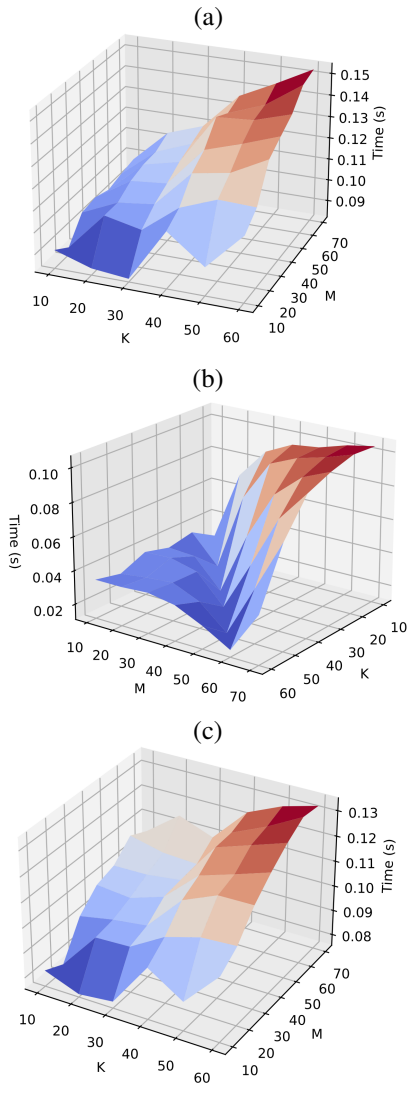

Source: The authors.

Conclusions

By using ZF or M-MMSE combiners and under certain system and channel conditions, the system SE in UL of massive MIMO systems can be increased without limits, as revealed by Figure 1, but performance degradation arises when the number of users K grows with a fixed number of BS antennas M, *i.e.*, when system loading $\mathscr{L}$ increases. While the system SE grows under ZF and M-MMSE combiners/precoders at the same rate, it is not the same when the number of users' connections K grows. Indeed, numerical results (Figure 2) reveal that the system SE using ZF combiner under massive MIMO system starts to decrease very early, *i.e.*, for $\mathscr{L} \geq 0.47$, and fast in contrast to M-MMSE, in which continues to increase and eventually decay with the number of users, but slowly. Since MR combiner is a simple strategy for this problem, it does not take advantage of the increasing number of antennas in the BS, neither can do much as the number of users K increases.

When using *Max-min fairness* power allocation strategy, the numerical results in Figure 3 show an improvement in individual SEs, in the sense of improving the system fairness, but consequently reducing its sum-rate (system SE). Its seen by comparison that using EPA the system achieves more SE but with a cost of drop out several UEs, disconnecting such users from the system whatsoever.

The EE-SE trade-off analysis (Figure 4) revealed that each combiner/precoding reaches a different optimum (maximum) EE-SE point of operation with different number of antennas M, and again, as expected, in terms of performance, MMSE combiner/precoding leads, followed by ZF and MR at last with a very low system EE.

Finally, the time computational complexity of the proposed *Max-min fairness* PA allocation under the *bisection* procedure (Algorithm 1) and in under-loading $\mathscr{L} \leq 1$ scenarios have revealed that the MMSE and MR result in a similar time complexity as opposed to the ZF combiner in which has faster convergence but worst performance under full-loading $K = M$ scenarios.

Acknowledgments

The authors wish to thank the Laboratory of Telecommunication and Signal Processing (LTSP), State University of Londrina, and Fundação Araucária, Paraná, for the financial support.

References

ALI, A.; CARVALHO, E. D.; HEATH, R. W. Linear receivers in non- stationary massive MIMO Channels with visibility regions. *IEEE Wireless Communications Letters*, Piscataway, v. 8, n. 3, p. 885–888, Jun. 2019.

ANDERSEN, M.; DAHL, J.; VANDENBERGHE, L. *Cvxopt*: python software package for convex optimization. [S. l.]: CVXOPT, 2021. Available from: https://cvxopt.org/. Access in: Sep. 20, 2021.

BJORNSON, E.; HOYDIS, J.; SANGUINETTI, L. Massive MIMO networks: Spectral, energy, and hardware efficiency. *Foundations and Trends in Signal Processing*, [Netherlands], v. 11, n. 3/4, p. 154–655, 2017.

BJORNSON, E.; SANGUINETTI, L.; WYMEERSCH, H.; HOYDIS, J.; MARZETTA, T. L. Massive MIMO is a reality – what is next? five promising research directions for antenna arrays. *Digital Signal Processing*, Duluth, v. 94, p. 3-20, 2019.

BOYD, S.; VANDENBERGHE, L. *Convex optimization*. Cambridge: Cambridge University Press, 2004.

CARVALHO, E. de; ALI, A.; AMIRI, A.; ANGJELICHINOSKI, M.; HEATH JUNIOR, R. W. Non-stationarities in extra-large scale massive MIMO. *IEEE Wireless Communications*, New York, v. 27, n. 4, p. 74-80, 2020.

JENG-SHIANN, J.; INGRAM, M. A. Spherical-wave model for short-range mimo. *IEEE Transactions on Communications*, New York, v. 53, n. 9, p. 1534– 1541, Sep. 2005.

KWON, J.-H.; CHO, J.; YU, B.; LEE, S.; JUNG, I.; HWANG, C.; KO, Y.-C. Spectral and energy efficient power allocation for mimo broadcast channels with individual delay and QoS constraints. *Journal of Communications and Networks*, [*s. l.*], v. 22, n. 5, p. 390– 398, 2020.

LI, H.; CHENG, J.; WANG, Z.; WANG, H. Joint antenna selection and power allocation for an energy-efficient massive mimo system. *IEEE Wireless Communications Letters*, Piscataway, v. 8, n. 1, p. 257–260, 2019.

OLIVERAS MARTINEZ, A.; EGGERS, P.; CARVALHO, E. Geometry-based stochastic channel models for 5g: Extending key fea- tures for massive mimo. *In*: ANNUAL INTERNATIONAL SYMPOSIUM ON PERSONAL, INDOOR, AND MOBILE RADIO COMMUNICATIONS (PIMRC), 27., 2016, Valencia. *Proceedings* [. . .]. Valencia: IEEE, 2016.p. 1–6.

PAYAMI, S.; TUFVESSON, F. Channel measurements and analysis for very large array systems at 2.6 ghz. *In*: EUROPEAN CONFERENCE ON ANTENNAS AND PROPAGATION (EUCAP), 6., 2012, Prague. *Proceedings* [. . .]. Prague: IEEE, 2012. P. 433–437.

SALH, A.; SHAH, N. S. M.; AUDAH, L.; ABDULLAH, Q.; JABBAR, W. A.; MOHAMAD, M. Energy-efficient power allocation and joint user association in multiuser-downlink massive mimo system. *IEEE Access*, Piscataway, v. 8, p. 1314 – 1326, Dec. 2019.

SANGUINETTI, L.; BJORNSON, E.; HOYDIS, J. Towards massive mimo 2.0: understanding spatial correlation, interference suppression, and pilot contamination. *IEEE Transactions on Communications*, New York, v.68, n. 1, p. 232–257, Jan. 2020.

ZHENG, K.; OU, S.; YIN, X. Massive mimo channel models: a survey. *International Journal of Antennas and Propagation*, Cairo, v. 2014,p. 1- 10, 2014.

ZHOU ZHOU, X. G.; FANG, J.; CHEN, Z. Spherical wave channel and analysis for large linear array in los conditions. *IEEE Globecom Workshops (GC Wkshps)*, San Diego, p. 1–6, Dec. 2015.

Received: June 8, 2021
Accepted: May 29, 2022
Published: June 3, 2022